Phase Unwrapping via Graph Cuts ⋆

José M. Bioucas-Dias[1] and Gonçalo Valadão[2]

[1] Instituto de Telecomunicações - Instituto Superior Técnico,
Av. Rovisco Pais, 1049-001 Lisboa, PORTUGAL
Phone: 351 21 8418466 Email: bioucas@lx.it.pt
[2] ICIST - Instituto Superior Técnico,
Av. Rovisco Pais, 1049-001 Lisboa, PORTUGAL
Phone: 351 21 8418336 Email: gvm@civil.ist.utl.pt

Abstract. This paper presents a new algorithm for recovering the absolute phase from modulo-2π phase, the so-called phase unwrapping (PU) problem. PU arises as a key step in several imaging technologies, from which we emphasize interferometric SAR and SAS, where topography is inferred from absolute phase measurements between two (or more) antennas and the terrain itself. The adopted criterion is the minimization of the L^p norm of phase differences [1], [2], usually leading to computationally demanding algorithms. Our approach follows the idea introduced in [3] of an iterative binary optimization scheme, the novelty being the casting onto a graph max-flow/min-cut formulation, for which there exists efficient algorithms. That graph formulation is based on recent energy minimization results via graph-cuts [4]. Accordingly, we term this new algorithm PUMF (for phase unwrapping max-flow). A set of experimental results illustrates the effectiveness of PUMF.

1 Introduction

Phase is an important property of many classes of signals [5]. For instance, interferometric SAR (InSAR) uses two or more antennas to measure the phase between the antennas and the terrain; the topography is then inferred from the difference between those phases [6]. In magnetic resonance imaging (MRI), phase is used, namely, to determine magnetic field deviation maps, which are used to correct echo-planar image geometric distortions [7]. In optical interferometry, phase measurements are used to detect objects shape, deformation, and vibration [8].

In all the examples above, in spite of phase being a crucial information, the acquisition system can only measure phase modulo-2π, the so-called principal phase value, or wrapped phase. Formally, we have

$$\phi = \psi + 2k\pi, \tag{1}$$

where ϕ is the true phase value (the so-called absolute value), ψ is the measured (wrapped) modulo-2π phase value, and $k \in \mathbb{Z}$ an integer number of wavelengths [2].

Phase unwrapping (PU) is the process of recovering the absolute phase ϕ from the wrapped phase ψ. This is, however, an ill-posed problem, if no further information is added. In fact, an assumption taken by most phase unwrapping algorithms is that the absolute value of phase differences between neighbouring pixels is less than π, the so-called Itoh condition [9]. If this assumption is not violated, the absolute phase can be easily determined, up to a constant. Itoh condition might be violated if the true phase surface is discontinuous, or if only a noisy version of the wrapped phase is available. In either cases, PU becomes a very difficult problem, to which much attention has been devoted [2], [3].

⋆ This work was supported by the Fundação para a Ciência e Tecnologia, under the projects POSI/34071/CPS/2000 and PDCTE/CPS/49967/2004.

Phase unwrapping approaches belong to one of these following classes: path following [10], minimum L^p norm [1], Bayesian [11], and parametric modelling [12].

Path following algorithms apply line integration schemes over the wrapped phase image, and basically rely on the assumption that Itoh condition holds along the integration path. Wherever that condition is not met, different integration paths may lead to different unwrapped phase values. Techniques employed to handle these inconsistencies include the so-called *residues branch cuts* [10] and *quality maps* [2].

Minimum norm methods exploit the fact that the differences between absolute phases of neighbour pixels, are equal to the wrapped differences between correspondent wrapped phases, if Itoh condition is met. Thus, these methods try to find a phase solution ϕ for which L^p norm of the difference between absolute phase differences and wrapped phase differences (so a second order difference) is minimized. This is, therefore, a global minimization in the sense that all the observed phases are used to compute a solution. With $p = 2$ we have a least squares method [13]. The exact solution with $p = 2$ is developed in [3] using network programming techniques. An approximation to the least squares solution can be obtained by relaxing the discrete domain $\mathbb{Z}^{MN}$ to $\mathbb{R}^{MN}$ and applying FFT or DCT based techniques [3]. A drawback of the L^2 norm is that this criterion tends to smooth discontinuities, unless they are provided as binary weights. L^1 norm performs better than L^2 norm in what discontinuity preserving is concerned. Such a criterion has been solved by Flynn [14] and Costantini [15], using network programming. With $0 \leq p < 1$ the ability of preserving discontinuities is further increased at stake, however, of highly complex algorithms.

The Bayesian approach relies on a data-observation mechanism model, as well as a prior knowledge of the phase to be modelled. For instance in [16], a non-linear optimal filtering is applied, while in [17] an InSAR observation model is considered, and is taken into account not only the image phase, but also the *backscattering coefficient* and *correlation factor* images, which are jointly recovered from InSAR image pairs.

Finally, parametric algorithms constrain the unwrapped phase to a parametric surface. Low order polynomial surfaces are used in [12]. Very often in real applications just one polynomial is not enough to describe accurately the complete surface. In such cases the image is partitioned and different parametric models are applied to each partition [12].

1.1 Proposed approach

This paper proposes a new phase minimum L^p norm unwrapping algorithm, that minimizes the L^p norm of the complete set of phase differences between neighbour pixels, with the additional constraint of being 2π-congruent with wrapped phases.

The integer optimization problem we are led to is solved by a series of binary elementary optimizations as presented in [3] for the $\mathbb{Z}\pi$M algorithm. The present approach casts, however, the optimization problem as a max-flow/min-cut calculation on a certain graph, building on energy minimization results presented in [4]. The developed algorithm is valid for $p \geq 1$. Accordingly, we call the method to be presented, the PUMF algorithm (for PU-max-flow).

2 Problem formulation

Adopting the representation used in [3], Fig.1 shows a pixel and its four neighbours along with the variables h and v signalling horizontal and vertical discontinuities respectively.

The L^p norm of the difference between neighbouring pixels phases, 2π-congruent with wrapped phases, is given by

$$E(\mathbf{k}|\boldsymbol{\psi}) = \sum_{ij \in \mathbb{Z}_1} \left|\Delta\phi_{ij}^h\right|^p \overline{v}_{ij} + \left|\Delta\phi_{ij}^v\right|^p \overline{h}_{ij}, \tag{2}$$

[3] Where M and N are the number of lines and columns respectively.

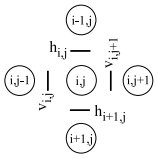

Fig. 1. Representation of the pixel (i,j) and its first order neighbours along with the variables h and v signalling horizontal and vertical discontinuities respectively.

where $(\cdot)^h$ and $(\cdot)^v$ denotes pixel horizontal and vertical differences given by

$$\Delta\phi_{ij}^h = \left[2\pi(k_{ij} - k_{ij-1}) - \Delta\psi_{ij}^h\right],\ k \in \mathbb{Z} \tag{3}$$

$$\Delta\phi_{ij}^v = \left[2\pi(k_{ij} - k_{i-1j}) - \Delta\psi_{ij}^v\right],\ k \in \mathbb{Z} \tag{4}$$

$$\Delta\psi_{ij}^h = \psi_{ij-1} - \psi_{ij} \tag{5}$$

$$\Delta\psi_{ij}^v = \psi_{i-1j} - \psi_{ij}, \tag{6}$$

with $p \geq 0$, ψ being the wrapped (observed) phase, $\overline{h}_{ij} = 1 - h_{ij}$ and $\overline{v}_{ij} = 1 - v_{ij}$ $(h_{ij}, v_{ij} \in \{0,1\})$ being binary horizontal and vertical discontinuities respectively, and $(i,j) \in \mathbb{Z}_1$ where $\mathbb{Z}_1 = \{(i,j) : i = 1,\ldots,M,\ j = 1,\ldots,N\}$, and with M and N denoting the number of lines and columns respectively (*i.e.*, the usual image pixel indexing 2D grid).

Our purpose is to find the integer image $\mathbf{k}$ that minimizes energy (2), $\mathbf{k}$ being such that $\boldsymbol{\phi} = 2\pi\mathbf{k} + \boldsymbol{\psi}$, where $\boldsymbol{\phi}$ is the estimated unwrapped image; $\mathbf{k}$ is the so-called *wrap-count* image. To achieve this goal, we compute a series of graph flow calculations for which efficient max-flow/min-cut algorithms exist.

3 Minimizing E by a Sequence of Binary Optimizations

The following lemma, taken from [3], assures that if the minimum of $E(\mathbf{k}|\boldsymbol{\psi})$ is not yet reached, then there exists a binary image $\delta\mathbf{k}$ (*i.e.*, the elements of $\delta\mathbf{k}$ are all 0 or 1) such that $E(\mathbf{k}+\delta\mathbf{k}|\boldsymbol{\psi}) < E(\mathbf{k}|\boldsymbol{\psi})$.

Lemma 1 *Let* $\mathbf{k}_1$ *and* $\mathbf{k}_2$ *be two wrap-count images such that*

$$E(\mathbf{k_2}|\boldsymbol{\psi}) < E(\mathbf{k_1}|\boldsymbol{\psi}). \tag{7}$$

Then there exists a binary image $\delta\mathbf{k}$ *such that*

$$E(\mathbf{k_1} + \delta\mathbf{k}|\boldsymbol{\psi}) < E(\mathbf{k}_1|\boldsymbol{\psi}). \tag{8}$$

Proof. The proof follows the same line of the one given in the appendix of [3] for $p = 2$, using the convexity of $|x|^p$ with respect to x, for $p \geq 1$.

According to Lemma 1, we can iteratively compute $\mathbf{k}^{t+1} = \mathbf{k}^t + \delta\mathbf{k}$, where $\delta\mathbf{k} \in \{0,1\}^{MN}$ minimizes $E(\mathbf{k}^t + \delta\mathbf{k}|\boldsymbol{\psi})$, until the the minimum energy is reached.

3.1 Mapping Binary Optimizations onto Graph Min-Cuts

Let $k_{ij}^{t+1} = k_{ij}^t + \delta k_{ij}^t$ be the wrap-count at time $t+1$ and pixel (i,j). Introducing k_{ij}^{t+1} into (3) and (4), we obtain, respectively,

$$\Delta\phi_{ij}^h = \left[2\pi(k_{ij}^{t+1} - k_{ij-1}^{t+1}) - \Delta\psi_{ij}^h\right] \tag{9}$$

$$\Delta\phi_{ij}^v = \left[2\pi(k_{ij}^{t+1} - k_{i-1j}^{t+1}) - \Delta\psi_{ij}^v\right]. \tag{10}$$

After some simple manipulation, we get

$$\Delta\phi_{ij}^h = \left[2\pi(\delta k_{ij}^t - \delta k_{ij-1}^t) + a^h\right] \tag{11}$$

$$\Delta\phi_{ij}^v = \left[2\pi(\delta k_{ij}^t - \delta k_{i-1j}^t) + a^v\right], \tag{12}$$

where $a^h = 2\pi(k_{ij}^t - k_{ij-1}^t) - \Delta\psi_{ij}^t$, and $a^v = 2\pi(k_{ij}^t - k_{i-1j}^t) - \Delta\psi_{ij}^t$. Now introducing (11) and (12) into (2), we can rewrite energy $E(\mathbf{k}|\boldsymbol{\psi})$ as a function of binary variables δk_{ij}^t, *i.e.*,

$$E(\mathbf{k}|\boldsymbol{\psi}) = \sum_{ij\in\mathbb{Z}_1} \underbrace{\left|2\pi(\delta k_{ij}^t - \delta k_{ij-1}^t) + a^h\right|^p \overline{v}_{ij}}_{E_h^{ij}(x_{ij-1},x_{ij})} + \underbrace{\left|2\pi(\delta k_{ij}^t - \delta k_{i-1j}^t) + a^v\right|^p \overline{h}_{ij}}_{E_v^{ij}(x_{i-1j},x_{ij})}, \tag{13}$$

where $x_{ij} = \delta k_{ij}^t$.

For simplicity, let us denote for a moment terms E_h^{ij} and E_v^{ij} by $E^{ij}(x_k, x_l)$. We have thus, $E^{ij}(0,0) = |a|^p\,\overline{d}_{ij}$, $E^{ij}(1,1) = |a|^p\,\overline{d}_{ij}$, $E^{ij}(0,1) = |2\pi + a|^p\,\overline{d}_{ij}$, and $E^{ij}(1,0) = |-2\pi + a|^p\,\overline{d}_{ij}$, where a represents a_h or a_v and $\overline{d}_{ij}$ represents $\overline{h}_{ij}$ or $\overline{v}_{ij}$.
So, we also have $E^{ij}(0,0)+E^{ij}(1,1) = 2\,|a|^p\,\overline{d}_{ij}$, and $E^{ij}(0,1)+E^{ij}(1,0) = (|-2\pi + a|^p + |2\pi + a|^p)\,\overline{d}_{ij}$. For $p \geq 1$, terms $E(x_k, x_l)$ verify $E^{ij}(0,0) + E^{ij}(1,1) \leq E^{ij}(0,1) + E^{ij}(1,0)$, this following from the convexity of $E(\mathbf{k}|\boldsymbol{\psi})$.

We are now in conditions of using Theorem 4.1 stated in [4]:

Theorem($\mathcal{F}^2$ theorem) 1 *Let E be a function of n binary variables from the class $\mathcal{F}^2$, i.e.,*

$$E(x_1, ..., x_n) = \sum_i E^i(x_i) + \sum_{i<j} E^{ij}(x_i, x_j). \tag{14}$$

Then E is graph-representable if and only if each term E^{ij} satisfies the inequality

$$E^{ij}(0,0) + E(1,1)^{ij} \leq E^{ij}(0,1) + E^{ij}(1,0). \tag{15}$$

Proof. See the proof in [4].

From the above theorem we can now state that energy $E(\mathbf{k}|\boldsymbol{\psi})$ (2) is graph representable. In fact, it has the structure of function E in Theorem 1, with null one-variable terms. The inequality (15) was verified above.

The proof of the precedent theorem, presented in [4], shows how to construct that graph. First, build vertices and edges corresponding to each pair of neighbouring pixels, and then join these graphs together based on the additivity theorem also given in [4].

So, for each energy term E_h^{ij} and E_v^{ij} (see expression 13), we construct an "elementary" graph with four vertices $\{s, t, v, v'\}$, where $\{s, t\}$ represents source and the sink, common to all terms, and $\{v, v'\}$ represents the two pixels involved (v being the left (up) pixel and v' the right (down) pixel). Following very closely [4], we define a directed edge (v, v') with the weight $E(0,1) + E(1,0) - E(0,0) - E(1,1)$. Moreover, if $E(1,0) - E(0,0) > 0$ we define an edge (s, v) with the weight

Algorithm 1 (PUMF) Graph cuts based phase unwrapping algorithm.

Initialization: $\boldsymbol{k} \equiv \boldsymbol{k'} \equiv \mathbf{0}$, possible_improvement $\equiv 1$

while possible_improvement **do**
  Compute $E(0,0), E(1,1), E(0,1)$, and $E(1,0)$ {for every horizontal and vertical pixel pairs}.
  Construct elementary graphs and merge them to obtain the main graph.
  Compute the min-cut (S,T) {S- source set; T-sink set}.
  for all pixel (i,j) **do**
    if pixel $(i,j) \in S$ **then**
      $\boldsymbol{k'}_{i,j} = \boldsymbol{k}_{i,j} + 1$
    else
      $\boldsymbol{k'}_{i,j} = \boldsymbol{k}_{i,j}$ {remains unchanged}
    end if
  end for
  if $E(\mathbf{k'}|\boldsymbol{\psi}) < E(\mathbf{k}|\boldsymbol{\psi})$ **then**
    $\mathbf{k} = \mathbf{k'}$
  else
    possible_ improvement = 0
  end if
end while

$E(1,0) - E(0,0)$ or, otherwise, we define an edge (v,t) with the weight $E(0,0) - E(1,0)$. In a similar way for vertex v', if $E(1,1) - E(1,0) > 0$ we define an edge (s,v') with weight $E(1,1) - E(1,0) > 0$ or, otherwise, we define an edge (v',t) with the weight $E(1,0) - E(1,1)$. Fig. 2(a) shows an example where $E(1,0) - E(0,0) > 0$ and $E(1,0) - E(1,1) > 0$. Fig. 2(b) illustrates the complete graph obtained at the end.

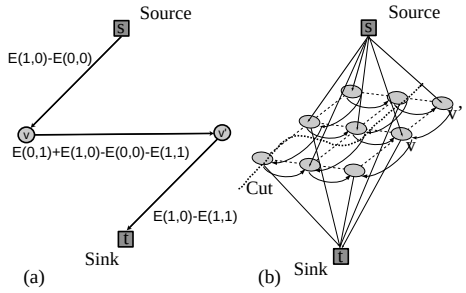

Fig. 2. (a) Elementary graph for a single energy term, where s and t represent source and sink respectively, and v and v' represent the two pixels involved in the energy term. In this case $E(1,0) - E(0,0) > 0$ and $E(1,0) - E(1,1) > 0$. (b) The graph obtained at the end results from adding elementary graphs.

In [4] it is shown that there is a one-to-one mapping, between the configuration of $(x_1, \ldots, x_n)$ and cuts leaving the source and the sink in disconnected components; furthermore, the cost of the cut is the value of the energy on that configuration. Therefore, minimizing the energy corresponds to computing the max-flow. As we have shown above, building on results from [3] and from [4], we can iteratively find an energy minimum through binary optimizations, based on max-flow calculation on a certain graph.

Algorithm 1 shows the pseudo-code for the Phase Unwrapping Max-Flow (PUMF) algorithm.

4 Experimental results

The results presented in this section were obtained by a MATLAB coding of the PUMF algorithm [max-flow was coded in C++ (see [18])].

Figs. 3(a) and 3(b) display two phase images to be unwrapped; they were synthesized from a Gaussian elevation height of 14π rad, and standard deviations $\sigma_i = 15$ and $\sigma_j = 10$ pixels. This synthesis consists of generating a pair of SAR complex images, given the desired absolute phase surface and pair coherence [19]; this is done according to the InSAR observation model adopted in [3]. The wrapped phase image is then obtained, by computing the product of one image by the complex conjugate of the other, and finally taking the argument. The correlation coefficient, $0 \leq \alpha \leq 1$, of the associated InSAR pairs is $\alpha = 1.0$ and $\alpha = 0.8$ respectively. The latter value is low enough to induce a large number of phase jumps, making the unwrapping a very difficult task. Figs. 3(c) and 3(d) show the corresponding unwrapped surfaces by PUMF with $p = 2$. We can see that in a few iterations (eight) PUMF successfully accomplishes the unwrapping.

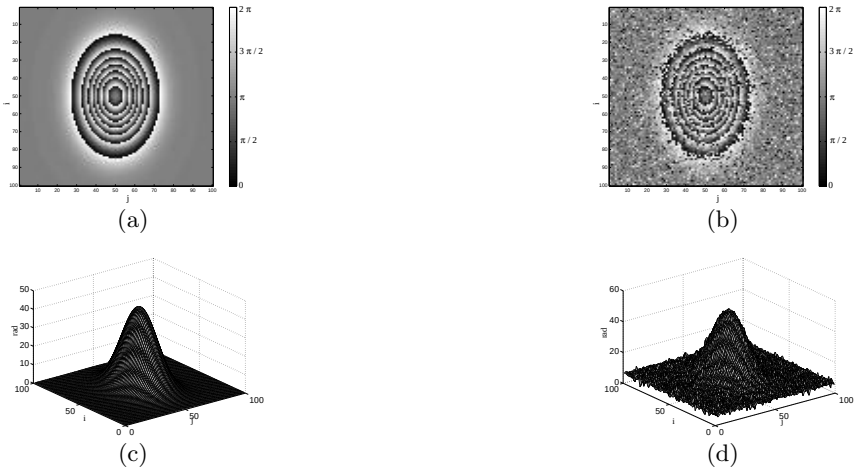

Fig. 3. (a) Wrapped phase image (rad) from a Gaussian absolute phase surface of height 14π rad and standard deviations $\sigma_i = 15$ and $\sigma_j = 10$. The correlation coefficient of the associated pair is $\alpha = 1.0$. (b) The same as in the previous figure but with $\alpha = 0.8$. (c) Image in (a) unwrapped by PUMF (7 iterations). (d) Image in (b) unwrapped by PUMF (8 iterations).

Fig. 4(a) shows a wrapped phase image analogous to 3(a), but now the original phase corresponds to a (simulated) InSAR acquisition for a (real) high-relief mountainous area inducing, therefore, many discontinuities and posing a very difficult PU problem. Figure 4(b) contains a, commonly called, quality map, which was supplied as an input discontinuity map to the algorithm. This quality map labels each pixel as 0 or 1 according, respectively, to whether there is, or there is not, a discontinuity; it was obtained by combining a mask, signing the top and the bottom (black) regions as discontinuities (artifacts arising from relief shadows), with a binary thresholded [2] image of correlation of the InSAR pair.

Figure 4(c) shows the unwrapped surface by PUMF. It should be stressed that this is a very tough phase unwrapping problem. PUMF accomplished the unwrapping, taking 17 iterations, with $p = 1$. Such a low value of p parameter greatly enhances the ability of the algorithm, to handle discontinuities. The excellent accuracy of this unwrapping is given by its error norm of 0.0970 (squared rads). The error norms obtained with the algorithms FMD and LPN0, the best unwrapping tech-

niques known to date [2], were 0.0986 and 0.1264 respectively, which shows the outperforming accuracy of PUMF in this PU problem [4]. Figure 4(d) shows the original surface.

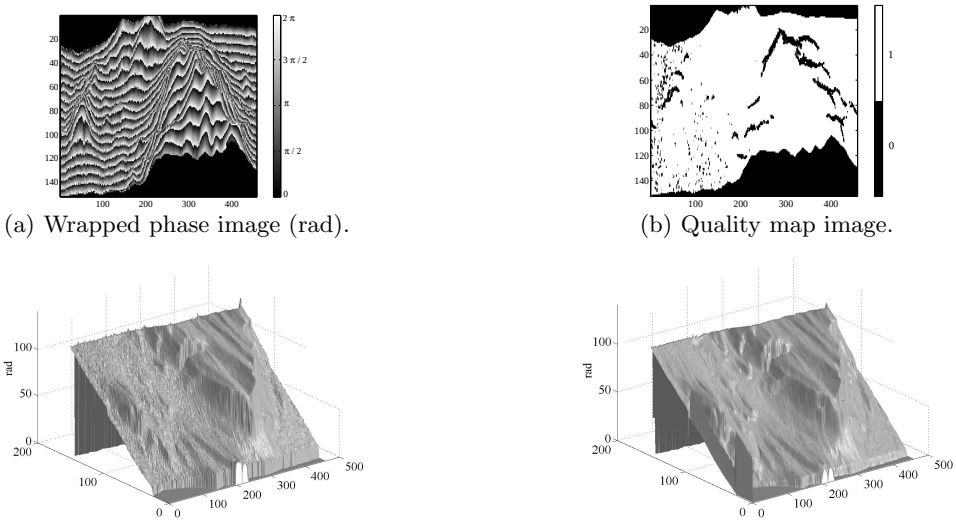

(a) Wrapped phase image (rad). (b) Quality map image.

(c) Image in (a) unwrapped by PUMF with p=1. (d) Original surface.

Fig. 4. PUMF unwrapping of simulated InSAR data (distributed with book [2]) for Long's Peak, Colorado.

5 Concluding remarks

We developed [5] a new graph cuts based phase unwrapping algorithm, in the vein of the minimum L^p norm class of PU algorithms, with $p \geq 1$. An iterative binary optimization scheme was adopted from $\mathbb{Z}\pi$M algorithm [3], and the results on energy minimization from [4] were applied, to perform the optimization, casting it on a series of graph max-flow/min-cut computations. Although we have not addressed the noise problem explicitly, PUMF is able to deal with discontinuities, in some cases even when their locations are unknown. In a set of experiments, the proposed PUMF algorithm competes with state-of-the-art methods. The performance of PUMF for $p < 1$ (with correspondingly enhanced discontinuities handling), is an issue to be addressed in the future. An exhaustive benchmarking with existing phase unwrapping algorithms also should be done.

References

1. D. Ghiglia and L. Romero. Minimum L^p norm two-dimensional phase unwrapping. *Journal of the Optical Society of America*, 13(10):1999–2013, 1996.
2. D. Ghiglia and M. Pritt. *Two-Dimentional Phase Unwrapping. Theory, Algorithms, and Software.* John Wiley & Sons, New York, 1998.
3. J. Dias and J. Leitão. The $\mathbb{Z}\pi$M algorithm for interferometric image reconstruction in SAR/SAS. *IEEE Transactions on Image Processing*, 11:408–422, April 2002.

[4] The error norms were calculated over the subset (of the entire image) defined by the quality map, plus a one pixel erosion in order to cut-off mask border pixels that usually have problems.

[5] The authors acknowledge Vladimir Kolmogorov for the max-flow/min-cut C++ code made available on the web.

4. V. Kolmogorov and R. Zabih. What energy functions can be minimized via graph cuts? *IEEE Transactions on Pattern Analysis and Machine Intelligence*, 26(2):147–159, February 2004.
5. A. V. Oppenheim and J. S. Lim. The importance of phase in signals. *Proceedings of the IEEE*, 69(5):529–541, May 1981.
6. P. Rosen, S. Hensley, I. Joughin, F. LI, S. Madsen, E. Rodriguez, and R. Goldstein. Synthetic aperture radar interferometry. *Proceedings of the IEEE*, 88(3):333–382, March 2000.
7. P. Jezzard and R. Balaban. Correction for geometric distortion in echo-planar images from B_0 field variations. *Magnetic Resonance in Medicine*, 34:65–73, 1995.
8. S. Pandit, N. Jordache, and G. Joshi. Data-dependent systems methodology for noise-insensitive phase unwrapping in laser interferometric surface characterization. *Journal of the Optical Society of America*, 11(10):2584–2592, 1994.
9. K. Itoh. Analysis of the phase unwrapping problem. *Applied Optics*, 21(14), 1982.
10. R. Goldstein, H. Zebker, and C. Werner. Satellite radar interferometry: Two-dimensional phase unwrapping. In *Symposium on the Ionospheric Effects on Communication and Related Systems*, volume 23, pages 713–720. Radio Science, 1988.
11. G. Nico, G. Palubinskas, and M. Datcu. Bayesian approach to phase unwrapping: theoretical study. *IEEE Transactions on Signal Processing*, 48(9):2545–2556, Sept. 2000.
12. B. Friedlander and J. Francos. Model based phase unwrapping of 2-d signals. *IEEE Transactions on Signal Processing*, 44(12):2999–3007, 1996.
13. D. Fried. Least-squares fitting a wave-front distortion estimate to an array of phase-difference measurements. *Journal of the Optical Society of America*, 67(3):370–375, 1977.
14. T. Flynn. Two-dimensional phase unwrapping with minimum weighted discontinuity. *Journal of the Optical Society of America A*, 14(10):2692–2701, 1997.
15. M. Costantini. A novel phase unwrapping method based on network programing. *IEEE Transactions on Geoscience and Remote Sensing*, 36(3):813–821, May 1998.
16. J. Leitão. Absolute phase image reconstruction: A stochastic non-linear filtering approach. *IEEE Transactions on Image Processing*, 7(6):868–882, June 1997.
17. J. Dias and J. Leitão. Simultaneous phase unwrapping and speckle smoothing in SAR images: A stochastic nonlinear filtering approach. In *EUSAR'98 European Conference on Synthetic Aperture Radar*, pages 373–377, Friedrichshafen, May 1998.
18. Y. Boykov and V. Kolmogorov. An experimental comparison of min-cut/max-flow algorithms for energy minimization in vision. ieee transactions on pattern analysis and machine intelligence. *IEEE Transactions on Pattern Analysis and Machine Intelligence*, 26(9):1124–1137, February 2004.
19. C. Jakowatz, D. Wahl, P. Eichel, D. Ghiglia, and P. Thompson. *Spotlight-Mode Synthetic Aperture Radar: A Signal Processing Approach*. Kluwer Academic Publishers, Boston, 1996.